JOURNAL OF PHYSIOLOGY AND PHARMACOLOGY 2018, 69, 6, 979-994
www.jpp.krakow.pl | DOI: 10.26402/jpp.2018.6.14

S. ALZAHRANI[1], W. EZZAT[2], R.E. ELSHAER[3], A.S. ABD EL-LATEEF[4], H.M.F. MOHAMMAD[5,6], A.Y. ELKAZAZ[7,8], E. TORAIH[9,10], S.A. ZAITONE[11,12]

STANDARDIZED *TRIBULUS TERRESTRIS* EXTRACT PROTECTS AGAINST ROTENONE-INDUCED OXIDATIVE DAMAGE AND NIGRAL DOPAMINE NEURONAL LOSS IN MICE

[1]Pharmacology Department, Faculty of Medicine, University of Tabuk, Tabuk, Saudi Arabia; [2]Physiology Department, Faculty of Medicine, Ain Shams University, Cairo, Egypt; [3]Pathology Department, Faculty of Medicine, Al-Azhar University, Cairo, Egypt; [4]Department of Pharmacology, Faculty of Medicine, Al-Azhar University, Cairo, Egypt; [5]Department of Clinical Pharmacology, Faculty of Medicine, Suez Canal University, Ismailia, Egypt; [6]Central Laboratory, Center of Excellence in Molecular and Cellular Medicine (CEMCM), Suez Canal University, Ismailia, Egypt; [7]Department of Medical Biochemistry and Molecular Biology, Faculty of Medicine, Suez Canal University, Ismailia, Egypt; [8]Department of Medical Biochemistry and Molecular Biology, Faculty of Medicine, Port Daid University, Port Said, Egypt; [9]Genetics Unit, Department of Histology and Cell Biology, Faculty of Medicine, Suez Canal University, Ismailia, Egypt; [10]Molecular Laboratory, Center of Excellence of Molecular and Cellular Medicine, Suez Canal University, Ismailia, Egypt; [11]Department of Pharmacology and Toxicology, Faculty of Pharmacy, University of Tabuk, Tabuk, Saudi Arabia; [12]Department of Pharmacology and Toxicology, Faculty of Pharmacy, Suez Canal University, Ismailia, Egypt

Strong evidence proposes that brain oxidative DNA damage and microglia activation contribute to Parkinson's disease (PD) pathogenesis. Traditional therapeutic regimens for PD can only relieve the symptoms. *Tribulus terrestris* (*T. terrestris*), a flowering plant from family Zygophyllaceae, is used in traditional medicine for treating different disorders and exerts neuroprotective and antioxidant effects in experimental models. The current study attempted to test whether treatment with *T. terrestris* standardized extract (TTE) can improve motor dysfunction and alleviate rotenone induced oxidative DNA damage and neurotoxicity in mice. Six groups of male Swiss albino mice were utilized. Group (1) was the vehicle (oil) group, group 2 was the rotenone control group (1 mg/kg/48 hours, subcutaneously) for 9 times, groups 3 and 4 were injected with rotenone and treated with TTE (5 or 10 mg per kg, by oral gavage) for 17 days, groups 5 and 6 served as TTE (5 or 10 mg per kg) *per se* groups. Motor function was measured by the pole and the open-field tests. Then, mouse brains were dissected, one hemisphere was employed for biochemical assays and the other one was used in histopathological studies. Results demonstrated that TTE ameliorated the motor dysfunctions induced by rotenone as well as markers of inflammation and DNA damage (8-OHdG and MTH1 expression). Indicators of oxidative stress and upregulation of the microglia marker ($CD_{11}b$) were suppressed by the higher dose of TTE (10 mg per kg). Finally, the higher dose of TTE improved the Cresyl violet staining and tyrosine hydroxylase immunostaining in the substantia nigra. In summary, TTE ameliorated the locomotor dysfunction and dampened the DNA damage and oxidoinflammatory stress in rotenone-parkinsonian mice. These results suggest TTE as a potential candidate for neurodegenerative diseases.

Key words: *dopaminergic neurons, oxidative damage, Parkinson's disease, rotenone, Tribulus terrestris, inflammation, microglia, cyclooxygenase-2, nitric oxide synthase*

INTRODUCTION

Parkinson's disease (PD) is an age-related neurodegenerative disorder and the most prevalent movement disorder (1). The features of PD comprise resting tremors, rigidity, bradykinesia, autonomic dysfunction and sleep disturbance (2). Dopaminergic system dysfunction is essential in PD pathogenesis (3).

Rotenone is a crystalline isoflavone commonly used as an insecticide and pesticide. Rotenone inhibits systemic mitochondrial complex I activity, with subsequent behavioral deficits in rodents resembling PD (4-6). Mitochondrial dysfunction generates reactive oxygen species (ROS) that may result in damage to DNA, impaired neuronal function and death causing neurodegeneration (7-9) characterized by build-up of different types of genomic DNA damage (10).

Microglia are the resident immune cells in the brain and serve various functions such as reacting to injury to minimize tissue damage, encouraging repair and stimulating neuronal survival. Microglial activation has been identified in the substantia nigra (SN) of both patients and experimental PD models such as rotenone model (4, 11) and results in production of a variety of cytotoxic factors like ROS, pro-inflammatory cytokines and nitric oxide (NO) (12, 13). Oxidative stress and inflammation increase the probability of developing neurodegeneration (14).

The key product of DNA oxidation is 8-hydroxy-deoxyguanosine (8-OHdG), which results in transcriptional mutagenesis and the generation of mutated species of protein that contribute to PD pathogenesis (15, 16). Human and rodents have MTH1 enzyme that hydrolyzes oxidized purine nucleoside triphosphates, such as 8-oxo-2-deoxyguanosine triphosphate and 2-hydroxy-20-deoxyadenosine triphosphate to the monophosphate forms (17).

Cumulative evidence has shown that phytochemicals such as nutraceuticals can alleviate neurodegenerative diseases through multiple mechanisms (4, 18, 19). *T. terrestris* is a plant from family Zygophyllaceae grows in tropical regions (20). This plant was commonly utilized in traditional Indian and Chinese folk medicine for treating some disorders and may boost male sexual functions (21). *T. terrestris* and related species have antioxidant properties against experimentally induced oxidative stress (22, 23). The fruit of *T. terrestris* contains active ingredients such as phytoesteroides, flavnoids, alkaloids, glycosides, steroidal saponins of the furostanol type, which produce anti-inflammatory effects (24). These compounds inhibit prostaglandin biosynthesis, NO production and cyclooxygenase-2 (COX-2) activity (25). Harmine is a β-carboline alkaloid that represents one of the key components in *T. terrestris* that participates in the pharmacological activities. Harmine reportedly inhibits monoamine oxidase and supports increased brain dopamine levels (26). Modern research indicates that flavonoids and steroidal saponins with noticeable antiaging and anti-inflammatory activities of *T. terrestris* extract (TTE) are responsible for this pharmacological activity (27). Adverse effects of TTE are rare however, some users report an upset stomach or gynecomastia (28).

This study tested the neuroprotection provided by TTE against neurodegeneration in rotenone parkinsonian mice. The usefulness of TTE was determined through measuring striatal dopamine and investigating the integrity of SNpc dopaminergic neurons by histopathological and immunohistochemical methods. The mechanism of this putative neuroprotective effect was clarified by focusing on the antioxidant and anti-inflammatory activities of TTE.

MATERIALS AND METHODS

List of materials

Rotenone was purchased from Sigma-Aldrich (MO, USA) and dissolved in sun flower oil for systemic administration (29, 30). Commercial tablets containing 1000 mg standardized TTE (containing minimum 45% saponins) were purchased from Now Sports Co. (USA). Tablets were ground in a mortar, dissolved in distilled water and given by oral route for 17 days from day 1 until day 17 (31). Control mice received equivalent volume of distilled water orally for 17 days.

Mice and experimental conditions

This work was performed using forty-two adult male Swiss albino mice with an initial body weight equals 20 – 28 g. Mice were supplied by Moustafa Rashed Company (Giza, Egypt) and kept under standard conditions in a hygienic area and with a normal light/dark cycle. Mice were acclimatized for 10 days during which regular chow diets were replenished daily at 9 a.m. with food and tap water provided *ad libitum*.

The study was carried out in compliance with the Declaration of Helsinki. Approval of the experimental protocols was obtained from the research ethics committee at the Faculty of Pharmacy at Suez Canal University.

Study protocol

Groups containing 7 mice each were assigned in the following order:

Group I: Vehicle control group: mice in this group received 10 ml/kg vehicle (sunflower oil) by subcutaneous injection every 48 ± 2 h for nine times.

Group II: Experimentally parkinsonian group: mice in this group were subjected to induction of parkinsonism by receiving nine subcutaneous doses of rotenone (1 mg per kg) that were repeated each 48 ± 2 h (4).

Groups III and IV: rotenone + TTE (5 or 10 mg per kg) groups: Parkinsonism was induced by injection of rotenone (1 mg per kg / 48 ± 2 h, 9 doses) and mice received TTE (5 or 10 mg per kg, daily) (21, 22, 32, 33) from day 1 to day 17. Both control and rotenone groups (groups 1 and 2) received distilled water (12 ml per kg, by oral gavage) daily parallel to doses of TTE in groups 3 and 4. TTE and distilled water were administered by oral gavage.

Group V and VI: TTE *per se* groups: mice were injected with vehicle (sunflower oil, s.c.) every 48 ± 2 h for 9 times and concomitantly received TTE (5 or 10 mg per kg, daily). These groups served as drug control groups to highlight any changes in locomotor activity or the architecture of the SNpc due to the *per se* administration of *T. terrestris.*

Assessment of mouse motor performance

One day after the end of the therapeutic period (day 18), mice in the experimental groups were screened for motor activity using the following tests.

1. Pole test performance

Pole test is generally employed for the assessment of motor dysfunction after striatal dopamine depletion (34). Every mouse was placed facing upward on the top of a pole standing vertically (50-cm-long and 1 cm in diameter/made of wood) while the pole base was positioned in the mouse home cage and titled at 45° from the base of the cage to stand on a nearby wall. Mice were placed with their heads directed upwards on the upmost part and were forced to attempt descending the pole to enter the home cage. The time that mice spent descending the pole to the home cage (descending time in seconds) was recorded. The best performance among the 5 trials was utilized for comparison (35, 36).

2. Open-field performance

An arena made of plexiglass (60 × 60 cm) with 30-cm high surrounding walls was used for evaluation of non-forced ambulation in animal models (19, 37, 38). The floor of the arena was highlighted to form an 8 × 8 cm rectangular unit's pattern. A central zone was set as a 16 × 16 cm rectangle at the middle of the arena. The apparatus was cleaned between trials with water and soft tissues. Animals were placed independently into the arena center and a video was recorded for a 5-min period by a camera installed above the box. Then, videos were used to determine the behavioral indicators by a trained observer in a blinded manner. Horizontal movement (the total count of squares crossed by the mouse body) and the number of stops (the number of occasions the mouse stopped after a period of locomotion) were recorded. Furthermore, an activity index was defined as the whole count of squares crossed by mice in 5 min divided by the count of stops; this determines the length of a locomotor interval (6). Furthermore, the sum of entries and time consumed at the central zone were also determined as indicators for anxiety behavior (39, 40).

Brain tissue sampling

After motor behavior tests, mice were anesthetized by an intraperitoneal injection of ketamine (75 mg per kg) and killed *via* cervical dislocation. Next, the brains were collected and washed with ice-cold phosphate-buffered saline (PBS) and dissected midsagittally into two halves. One of the hemispheres (left one) was fixed overnight in 4% paraformaldehyde followed by paraffin embedding. Then, 4 µm sections were cut at the SN level and stained with hematoxylin-eosin (HE) or Cresyl violet. From each frozen right hemisphere, striata were isolated and weighed. Striata were homogenized in PBS using a teflon homogenizer, sonicated and centrifuged for a 15-min period at 2000 × g. Then, supernatants were aliquoted and frozen at –20°C for measuring dopamine and oxidation parameters. Otherwise, pieces from the striata were processed for measuring mRNA expression of the selected genes.

Histopathological studies and immunohistochemical analysis

Neurodegeneration was evaluated in H + E stained SNpc neurons by observing pyknotic neurons in each nigral section. Degenerating neurons were identified by morphological characteristics such as blebbing of plasma membranes, neurons with dark stain and shrinking of cytoplasm, vacuoles surrounding the neurons, variations in size, neurons with a three-cornered shape and condensed nuclei (41). Cresyl violet staining marks the Nissl substances in the cytoplasm of neurons. Microtome sections were stained by a 0.5% Cresyl violet solution for 10 min. Then, the sections were covered and checked under a light microscope. Neuronal morphology was examined in the whole surface of the SNpc at × 10. Imaging was done at × 40 and normal neurons were identified by visible nuclei and complete outlines.

Tissue sections were cut at 4-µm at the SN level and subjected to deparaffinization and rehydration and then handled to retrieve antigens with Tris-EDTA (pH = 9). Sections were incubated with rabbit anti-phospho-TH antibodies from R&D Systems (USA) overnight in a humidified chamber. This step was followed by adding biotinylated secondary antibodies to tissue sections for 60 min. A Power-Stain™ kit (Genemed Biotechnologies, CA, USA) was used to visualize the reaction and Mayer's hematoxylin was utilized for counterstaining. Immunostaining in the SNpc was imaged at × 400 and images were investigated to count TH positive neurons containing visible nuclei. Counting was done in a blinded manner.

Biochemical assays

1. Determination of striatal dopamine level

Dopamine levels are most commonly determined by enzyme-linked immunosorbent assay (ELISA) (4) HPLC (42) or intracerebral microdialysis (43). In the current study, samples were thawed at room temperature. A dopamine ELISA kit from Sun Red Bio Company (China) was utilized to estimate of the concentration in the striatal homogenate. Assays were performed according to the directions listed by the manufacturer.

2. Determination of striatal level of oxidative stress markers

The supernatants were utilized for measurement of malondialdehyde (MDA) and reduced glutathione (GSH) as well as the activity of catalase (CAT) and superoxide dismutase (SOD) by spectrophotometric kits (Biodiagnostic, Co., Cairo, Egypt). MDA was measured in the homogenate by determining thiobarbituric acid reactive species following a previous method (44). GSH was also determined following a previously designated method (45). This method relies on the reaction between Ellman's reagent and GSH to produce a yellowish compound that has a distinctive absorption at 412 nm. Finally, SOD activity was proportional to the degree of impairment of the nitroblue tetrazolium reduction by superoxide (46). CAT activity was estimated through determination of the breakdown of H_2O_2 (47). Quantitative measurement of the reduction in the absorbance was measured at 240 nm.

3. Determination of striatal mRNA expression for $CD_{11}b$, inducible nitric oxide synthase and cyclooxygenase-2

An SV total RNA isolation system from Promega (Madison, USA) was used to extract total RNA from the homogenate. Content and purity of RNA were estimated by a UV-spectrophotometer. Complementary DNA (cDNA) synthesis was done using a 1 µg RNA sample. Then, a SuperScript III First-Strand Synthesis System (#K1621, USA) was used according to instructions of the manufacturer. Real-time quantitative PCR was done through the following steps. First, amplification and analysis were completed using Applied Biosystem software (StepOne™, USA). The designed primer sequences for $CD_{11}b$ (a marker for microglia cells), inducible nitric oxide synthase (iNOS) (48) COX-2 (49) and GADPH (50) are illustrated in *Table 1*. Second, calculation of data was performed employing the v1·7 sequence detection program (PE Biosystems, USA). The comparative Ct method was used to identify the relative expression of the studied genes. Finally, normalizing data was done to β-actin and reported as the fold-change over the control group.

Assays for DNA damage

1. DNA laddering assay

A Promega Wizard® Genomic DNA Purification kit (USA) was used for extraction of genomic DNA. A Nanodrop®

Table 1. Primers and annealing temperatures used in real-time PCR reactions.

Gene	Primers	Annealing temperature
COX-2	Forward: TGACAGTCCACCTACTTACAAT Reverse: CTCCACCAATGACCTGATA	50ºC
CD11b	Forward: ATGGACGCTGATGGCAATACC Reverse: TCCCCATTCACGTCTCCCA	55ºC
iNOS	Forward: TTCACCCAGTTGTGCATCGACCTA Reverse: TCCATGGTCACCTCCAACACAAGA	57ºC
GAPDH	Forward: AGAGGGAAATCGTGCGTGAC Reverse: ACGGCCAGGTCATCACTATTG	54ºC

spectrophotometer)NA-1000 UV/Vis, ThermoFisher (was employed for checking the strength and purity of DNA. Next, DNA was exposed to horizontal agarose gel electrophoresis as described previously (4). Then, visualization of the DNA ladder was done by the aid of a UV- trans-illumination.

2. Determination of 8-OHdG by an ELISA kit

Estimation of 8-OHdG was done using an ELISA kit from CUSABIO. The assay employed the quantitative sandwich enzyme immunoassay technique where 8-OHdG antibodies were pre-coated onto a microplate. Samples and standards were transferred into wells and any existing 8-OHdG was bound by the free antibody. Following removal of unbound substances, a biotin-conjugated antibody against 8-OHdG was added to the wells. Next, following the washing step, avidin-conjugated horseradish peroxidase was transferred to the wells. After a wash, substrate solution was added to the wells and the colour produced was proportional to the concentration of 8-OHdG. The colour development is stopped and the intensity of the colour is measured.

3. Real-time quantitative RT-PCR analysis for MTH1

Total RNA was extracted from brain tissue specimens obtained from each group using TRIzol reagent (Invitrogen, USA). cDNA synthesis was done employing RT reagent kit (Invitrogen, USA). Real-time quantitation of MTH1 mRNA was done using a lightcycler-Faststart DNA master SYBR green I Roche PCR kit in a Roche LightCycler 2.0 detection system following the manufacturer's protocol. MTH1 cDNA forward and reverse primers were: 5'-AAAGTGGTCTGAGCGTGGAT-3' and 5'-TCTTCTGAAGCAGGAGTGGG-3', respectively. GAPDH was selected as an endogenous control. The GADPH forward and reverse cDNA primers were 5'-GTTGTCTCCTGCGACTTCA-3' and 5'-TGGTCCAGGGTTTCTTACTC-3', respectively. The expression of each sample relative to the GAPDH control gene was calculated employing the comparative Ct method.

Statistical analyses

Data are demonstrated as mean ± SD and were analyzed using one-way analysis of variance (ANOVA) followed by Tukey's multiple-comparisons test. All probable comparisons were detected among the experimental groups. Statistical analysis was done applying the Statistical Package of the Social Sciences (SPSS) program and the GraphPad Prism software. Differences were considered statistically significant at $P < 0.05$.

RESULTS

Compared with vehicle-injected mice, rotenone treated mice spent 11-fold more time descending in the pole test (14.14 ± 4.26 versus 166.17 ± 43.33). Compared with rotenone treatment, TTE (5 or 10 mg/kg) treatment shortened the time to descend the pole in this test (166.17 ± 43.33 versus 17.6 ± 2.7 and 13.2 ± 4.26, *Fig. 1A*).

In the open-field test, rotenone injected mice showed impaired locomotor function; these mice crossed fewer squares and had a lower activity index than did vehicle (oil) treated mice (119.67 ± 39.16 versus 372.43 ± 54 squares and 8.29 ± 2.41 versus 26.27 ± 10.22, respectively, *Fig. 1B* and *1D*). However, the number of stops counted by the observer was not different between the rotenone group and vehicle group (*Fig. 1C*). Compared with treatment with rotenone, treatment with rotenone + TTE (10 mg per kg) significantly increased the count of traversed squares and the activity index ($P < 0.05$). The *per se* treatment with TTE at 5 or 10 mg/kg did not cause a difference in the measured parameters compared to the vehicle (number of squares 363.71 ± 49.03 and 394.86 ± 41.11 versus 372.43 ± 54), number of stops (15 ± 3.83 and 14.29 ± 3.03 versus 15.57 ± 5.57) and activity index (25.86 ± 8.31 and 28.86 ± 5.71 versus 26.27 ± 10.22).

By contrast, indicators of anxiety measured in the central zone revealed that compared to vehicle-treated mice, rotenone treated mice showed an increase in the number of entries or time spent within the central zone (4.57 ± 0.79 entries versus 7.67 ± 1.03 entries and time consumed within the central zone = 9.14 ± 1.05 s versus 13.57 ± 2.14 s, respectively). Furthermore, the rotenone + TTE (5 or 10 mg per kg) groups presented fewer entries than did the rotenone group (3.43 ± 1.13 and 3.83 ± 0.98 versus 7.67 ± 1.03 entries) and spent less time within the central zone than did the rotenone control group (mean = 7.14 ± 1.047 and 6.14 ± 3.2 s versus 13.57 ± 3.2 s). Importantly, compared with the vehicle control, *per se* treatment with TTE (5 or 10 mg/kg) did not produce a difference in the number of entries or time spent in the central zone (4.57 ± 0.79 entries versus 5.57 ± 0.98 and 4.71 ± 0.76 and 9.14 ± 1.05 s versus 9.43 ± 0.82 and 8.36 ± 1.02, respectively, *Fig. 1E* and *1F*).

Routine examination of histologic sections from the SNpc indicated that mice treated with sunflower oil (the vehicle) displayed normal neurons with large vesicular nuclei, pale eosinophilic cytoplasm and noticeable nucleoli (*Fig. 2A*). However, SNpc from rotenone group showed a mixture of normal and degenerated neurons in a ratio of 3:1 per high-power field. Degenerated SNpc neurons exhibited cytoplasmic vacuoles with irregular faint nuclei, or irregular pyknotic nuclei (*Fig. 2B*). Treatment with 5 or 10 mg/kg TTE caused improvements in the histopathological features and produced greater number of normal neurons and few degenerated neurons (*Fig. 2C* and *2D*). *Per se* treatment with 5 or 10 mg/kg TTE resulted in normal neurons with pale eosinophilic cytoplasm (*Fig. 2E* and *2F*). The mean percentage of pyknotic neurons in the study groups is shown in *Fig. 2G*.

Cresyl violet staining demonstrated that normal SNpc neurons exhibited clear distinct nuclear membranes in the vehicle group (*Fig. 3A*). However, the SNpc in rotenone group showed a mixture of normal and degenerated neurons, and degenerated neurons exhibited cytoplasmic vacuoles with irregular faint nuclei or irregular pyknotic nuclei (*Fig. 3B*). The SNpc in the groups treated with rotenone + TTE (5 or 10 mg/kg) showed normal neurons and few degenerated neurons (*Fig. 3C* and *3D*). The percentage of viable neurons after *per se* treatment with TTE (5 or 10 mg/kg) indicated no difference versus the vehicle control (*Fig. 3E* and *3F*). *Fig. 3G* shows that the percentage of viable neurons in the rotenone control group was significantly lower than the vehicle group. Rotenone + TTE (10 mg/kg) resulted in an increase in the percentage of viable neurons.

Immunohistochemical staining for nigral TH demonstrated strong cytoplasmic staining and normal neurons in oil group. By contrast, rotenone group showed some very strong positive staining in some normal neurons and a lack of staining in degenerated neurons. The SNpc from mice that received TTE 5 or 10 mg/kg revealed strong cytoplasmic TH immunostaining (*Fig. 4*). Furthermore, the TTE (5 or 10 mg/kg) *per se* groups showed strong cytoplasmic staining in SNpc neurons (*Fig. 4E* and *4F*). *Fig. 4G* shows that the rotenone group showed a lower percentage of TH-positive neurons than did the vehicle group while the rotenone + TTE (10 mg/kg) group showed a greater percentage of positive neurons than did the rotenone control group. *Per se* treatment with TTE (5 or 10 mg/kg) did not show a difference in percent of positive neurons in comparison with the vehicle control (*Fig. 4G*).

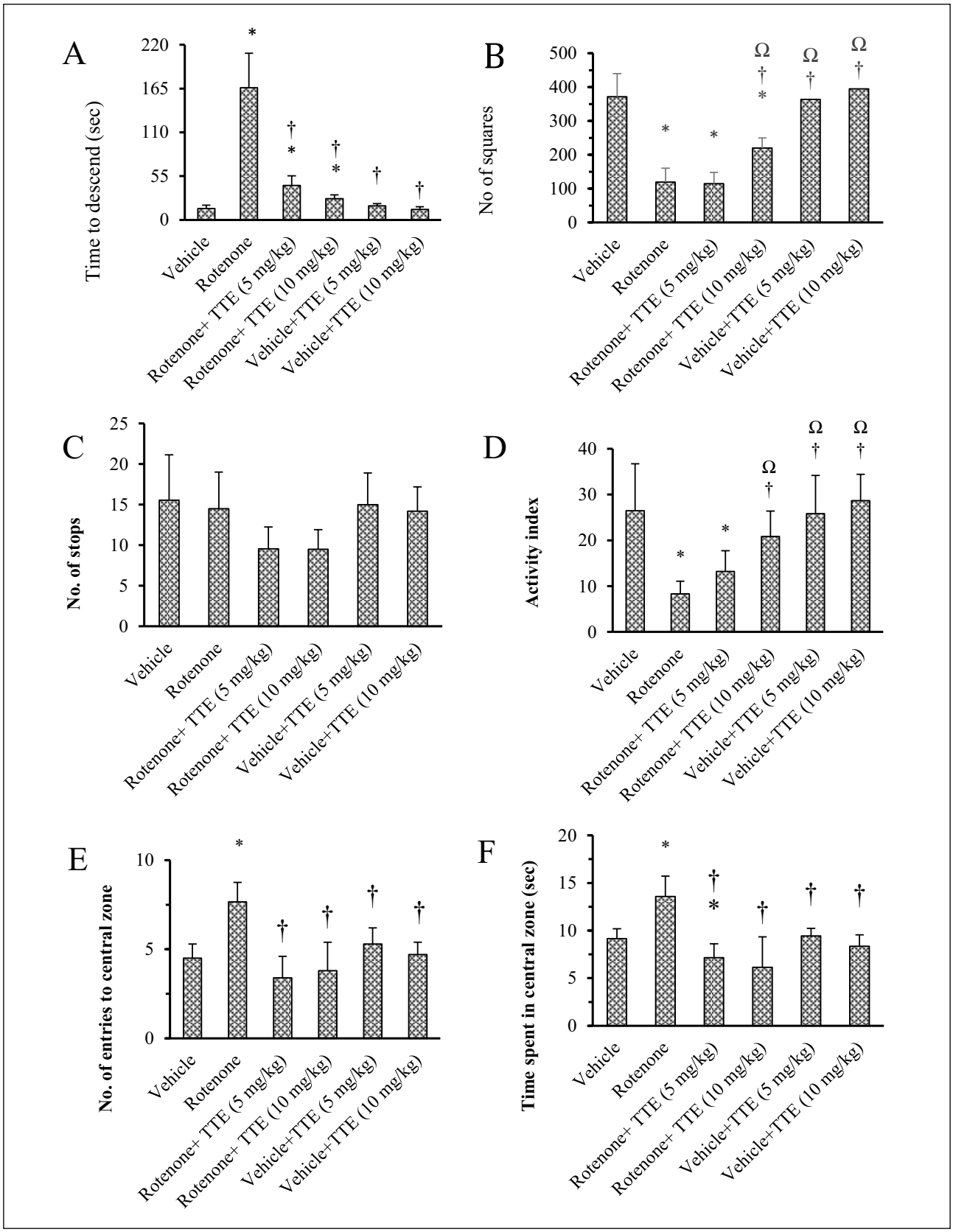

Fig. 1. Effect of *T. terrestris* extract on the mice performance in the pole test and the open-field test. (A): Time to descend in the pole test. Time to descend was calculated from the moment of putting the animal on the titled rod until it descends to its home cage (s). Naive mice were introduced individually into the open field arena and motor activity was monitored for 5 min, No. of squares (B), Number of stops (C), activity index (D), number of entries to the central zone (E) and time spent in the central zone (F). Activity index was calculated by dividing the No. of crossed squares by the No. of stops for each mouse. Data are means and SD and analyzed using one-way ANOVA followed by Tukey's test. P-value < 0.05 was set as the accepted level of significance. * Compared to vehicle group; † ompared to rotenone group, Ω compared to rotenone + TTE (5 mg/kg) group.

Biochemical analysis confirmed that rotenone-treated mice presented one-quarter (25%) of the striatal dopamine level in the vehicle- treated mice. Compared with treatment with rotenone, treatment with 10 mg/kg TTE -but not the low dose- significantly improved dopamine levels. Compared with treatment with the vehicle, *per se* treatment with TTE (5 or 10 mg/kg) did not show a

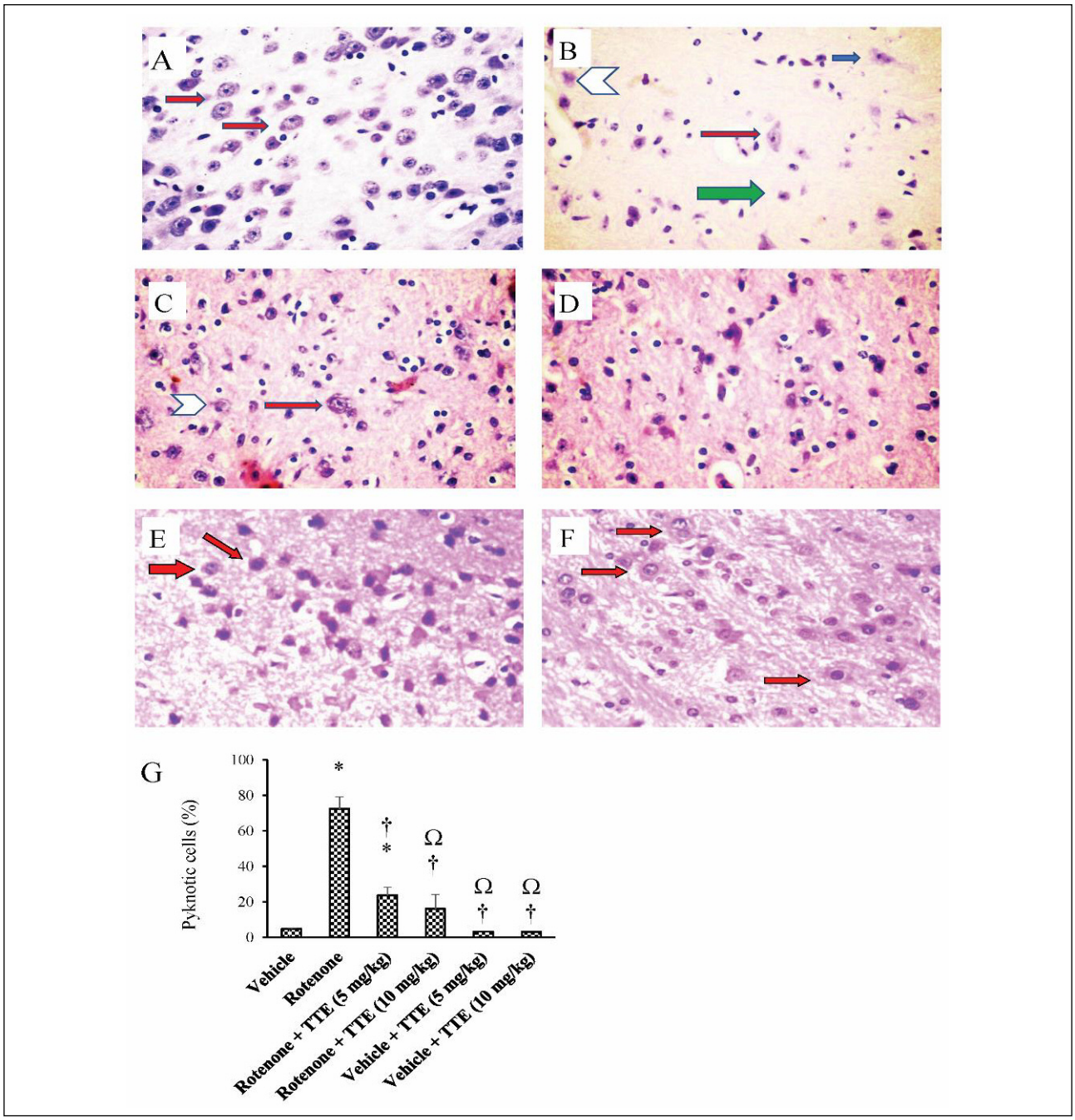

Fig. 2. Effect of *T. terrestris* extract (5 or 10 mg/kg) on the histopathologic picture of the substantia nigra of rotenone-parkinsonian mice. Photographs for sections from the substantia nigra pars compacta stained with hematoxylin and eosin. (A): Photograph from substantia nigra from mice treated with sunflower oil showing normal neurons (thin arrows) exhibiting large vesicular nuclei, prominent nucleoli and pale eosinophilic cytoplasm (H&E × 300). (B): Photographs from substantia nigra of rotenone group showing mixed normal neurons (thin arrows) and degenerated neurons in proportion 3:1 per high-power field, the degenerated neurons exhibit, cytoplasmic vacuoles wih irregular faint nuclei (arrow head), or irregular pyknotic nuclei (thick arrow). (C): Photograph from substantia nigra from rotenone group showing mixed normal neurons (thin arrow) and degenerated neuron (arrow head) (H&E × 300). (D): Photographs from substantia nigra from mice treated with rotenone + *T. terrestris* extract (10 mg per kg) showing normal neurons (thin arrows) and few degenerated neurons (H&E × 300). (E): and (F): Photographs for substantia nigra from mice groups received per se treatment with *T. terrestris* extract (5 or 10 mg per kg) showing normal neurons with large vesicular nuclei and prominent nucleoli (white arrows) (H&E × 400). (G): Column chare demonstrating the percent of pyknotic cells in the experimental groups. Data are mean ± SD and were analyzed using one-way ANOVA and Tukey's test. P-value < 0.05 was set as the accepted level of significance. * Compared to vehicle group, † compared to rotenone group, Ω compared to rotenone + TTE (5 mg/kg) group.

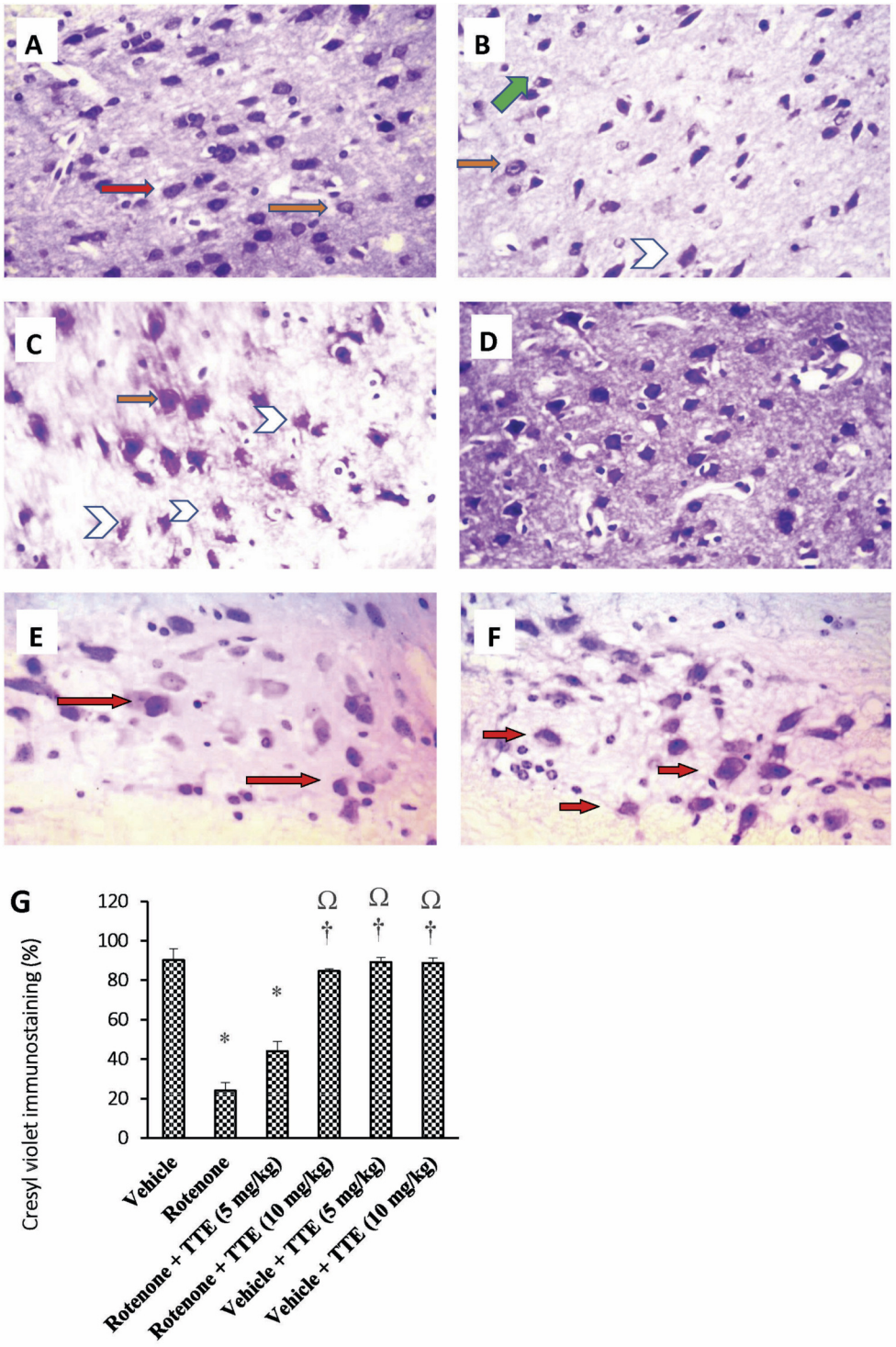

Fig. 3. Effect of *T. terrestris* on viability of neurons stained with Cresyl violet stain. Photomicrographs for sections from the substantia nigra pars compacta from the experimental groups. (A): Photograph from substantia nigra showing normal neurons, exhibit clear and distinct nuclear membrane (Cresyl violet × 300). (B): Photograph from substantia nigra form rotenone group showing mixed normal neurons (thin arrows) and degenerated neurons, the degenerated neurons exhibit, cytoplasmic vacuoles with irregular faint nuclei (arrow heads), or irregular pyknotic nuclei (thick arrow) (Cresyl violet × 300). (C): and (D): Photographs from substantia nigra of mice treated with *T. terrestris* extract (5 or 10 mg/kg), respectively, showing mixed normal neurons (thin arrows) and degenerated neurons, the degenerated neurons exhibit, cytoplasmic vacuoles with irregular faint nuclei (arrow head), or irregular pyknotic nuclei (thin arrow) (Cresyl violet × 400). Photograph from substantia nigra showing normal neurons (thin arrows) and few degenerated neurons (Cresyl violet × 300). (E): and (F): Photographs for substantia nigra from mice groups received *per se* treatment with *T. terrestris* extract (5 or 10 mg per kg) showing normal neurons (white arrows) (Cresyl violet × 400). (G): Column chare demonstrating the percent of viable neurons in the experimental groups. Data are mean ± SD and were analyzed using one-way ANOVA and Tukey's test. P-value < 0.05 was set as the accepted level of significance. * Compared to vehicle group, † compared to rotenone group, Ω compared to rotenone + TTE (5 mg/kg) group.

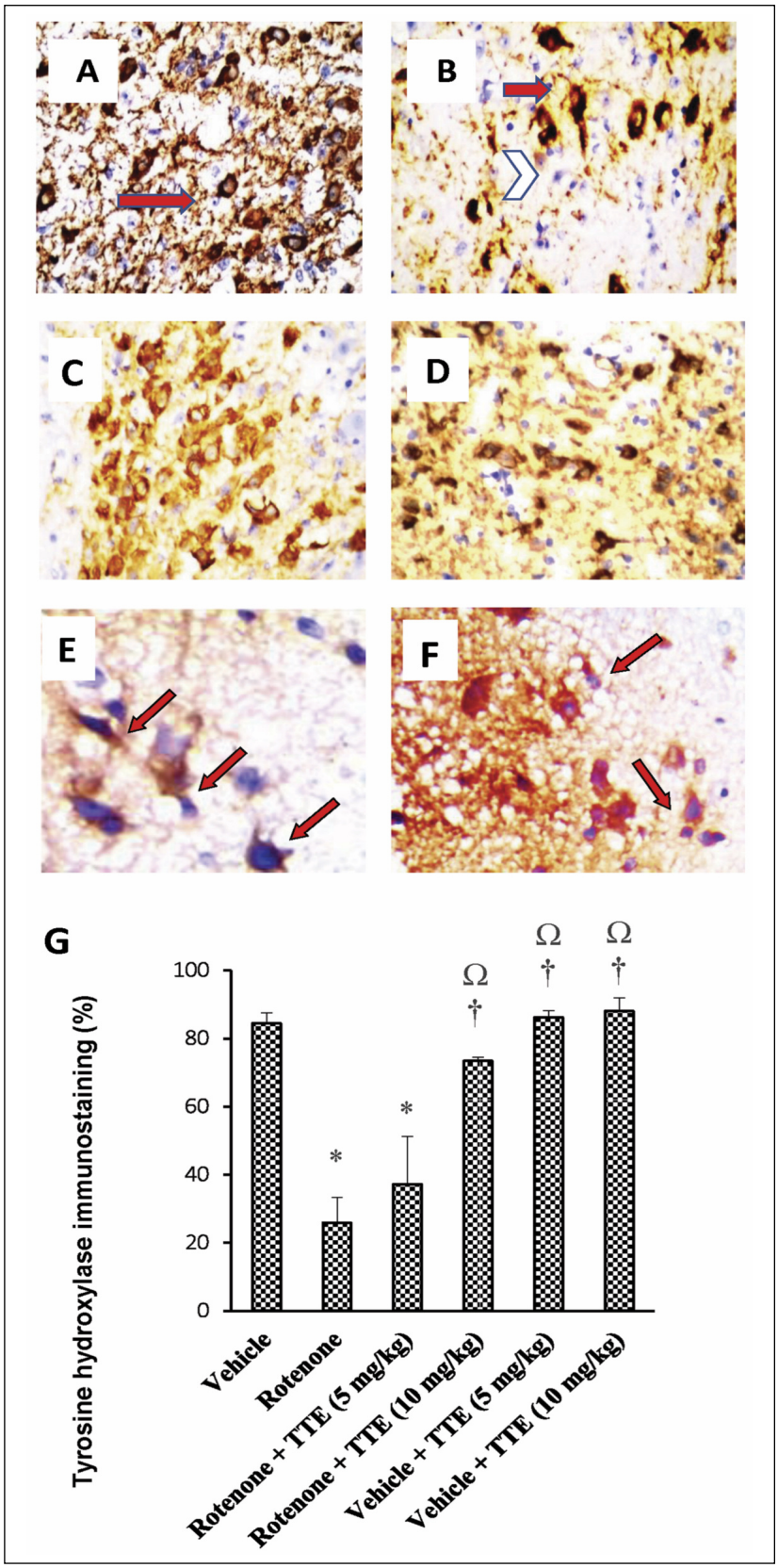

Fig. 4. Effect of *T. terrestris* extract on nigral immunohistochemical staining for tyrosine hydroxylase. Photographs for sections from the substantia nigra pars compacta immunostained for tyrosine hydroxylase. (A): Photograph from substantia nigra pars compacta in mice treated with sunflower oil showing strong cytoplasmic staining of the normal neurons with tyrosine hydroxylase (TH × 400). (B): A photograph for sections from rotenone group showing some very strong positive staining in normal neurons (red arrow) and a lack of staining showing degenerative neurons (blue arrow), (× 400). (C): A photograph from the substantia nigra showing strong cytoplasmic TH immunostaining in regenerated neurons and some degenerated neurons (TH × 400). (D): A photograph from the substantia nigra showing strong cytoplasmic TH immunostaining in most of regenerated neurons (TH × 400). (E): and (F): Photographs for substantia nigra from mice groups received *per se* treatment with *T. terrestris* extract (5 or 10 mg per kg) showing normal neurons (white arrows) (Cresyl violet × 400). (G): Column chart demonstrating TH immunostaining (%) in the experimental groups. Data are mean ± SD and were analyzed using one-way ANOVA and Tukey's test. P-value < 0.05 was set as the accepted level of significance. * Compared to vehicle group, † compared to rotenone group, Ω compared to rotenone + TTE (5 mg/kg) group.

difference in striatal dopamine levels (*Fig*. 5*A*). In addition, striatal mRNA expression of $CD_{11}b$, COX-2 and iNOS was upregulated in rotenone control group compared to that in the vehicle group. Compared to the rotenone group, the rotenone + TTE (10 mg/kg) group showed downregulated $CD_{11}b$ expression. However, the rotenone + TTE (5 or 10 mg/kg) groups displayed lower COX-2 (dose-dependent effect) and iNOS expression than did the rotenone control group. Compared with treatment with vehicle, *per se* treatment with TTE (5 or 10 mg/kg) did not produce a significant change in expression of these genes (*Fig*. 5*B-5D*).

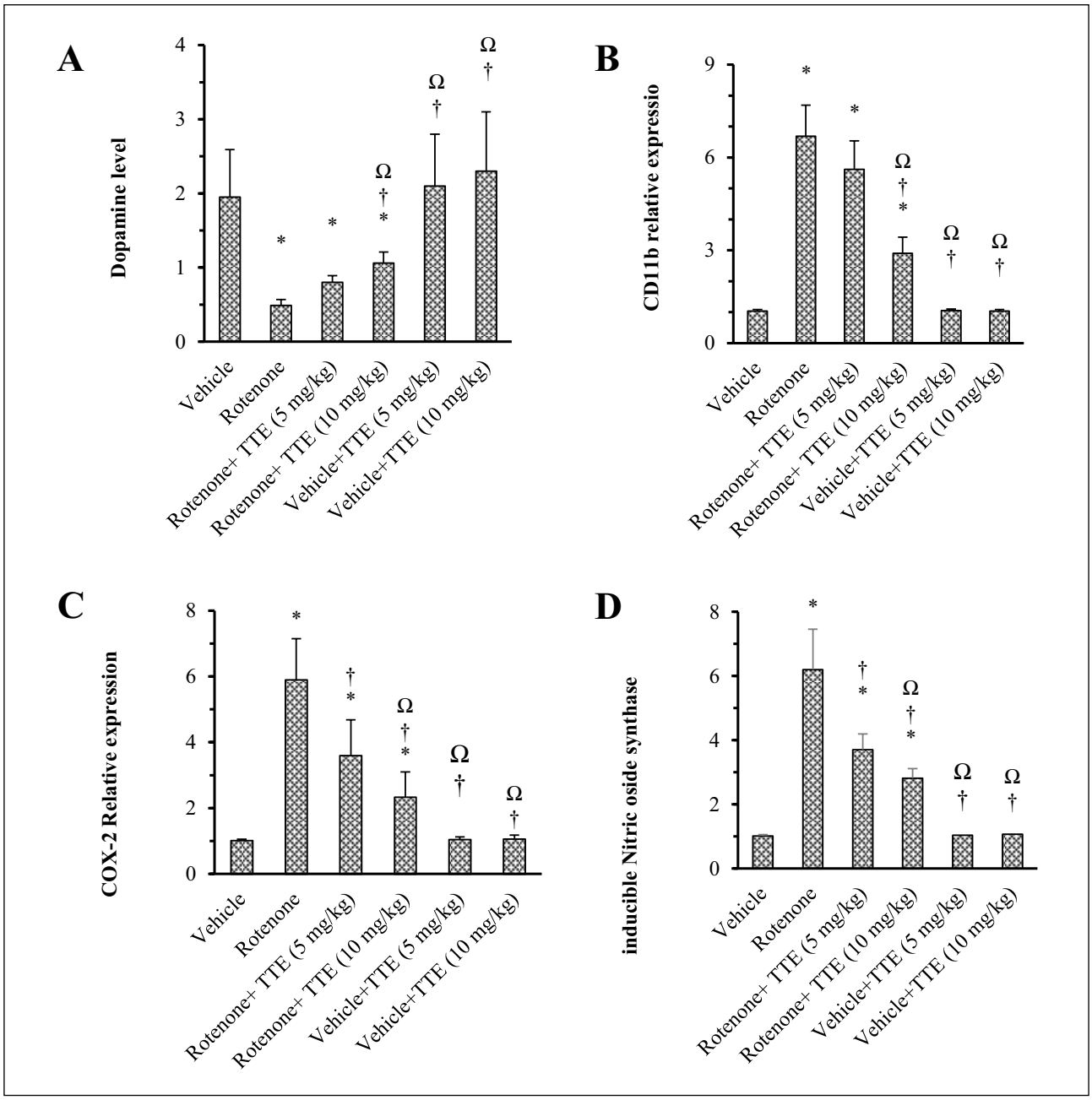

Fig. 5. Effect of *T. terrestris* extract (5 or 10 mg/kg) on striatal dopamine, mRNA expression of CD11b, cyclooxygenase-2 and iNOS in striata of mice. *T. terrestris* extract was given orally to mice daily for 17 days. Striatal level of dopamine (A), $CD_{11}b$ (B), cyclooxygenase-2 (C) and inducible nitric oxide synthase (D). CD11b: a marker for microglia in brain, COX-2: cyclooxygenase, iNOS: inducible nitric oxide synthase. Data are mean ± SD and analysis was performed by one-way ANOVA followed by Tukey's post-hoc test. P-value < 0.05 was set as the accepted level of significance. * Compared to vehicle group, † compared to rotenone group, Ω compared to rotenone + TTE (5 mg/kg) group.

Oxidative stress markers indicated greater MDA levels but lower GSH, SOD and CAT levels in the rotenone group than in the vehicle (oil) group. Only the high dose of TTE (10 mg/kg) ameliorated these markers; compared with the rotenone group, rotenone + TTE (10 mg/kg) group showed less MDA and more GSH, SOD activity and CAT activity. *Per se* treatment with TTE (5 or 10 mg/kg) resulted in a difference in these markers (*Fig. 6A-6D*).

Fig. 7 shows the DNA ladder for striatal specimens from the study groups. A DNA sample from the striata of the vehicle group showed intact DNA band while a sample from the rotenone group showed a greater level of laddering. Mice treated with TTE (10 mg/kg) presented a better quality DNA band than did mice treated with rotenone. Mice received *per se* treatment with TTE 5 or 10 mg per kg showed intact DNA bands (*Fig. 7A*). Striatal 8-OHdG concentration and MTH 1 expression showed significant increases in the rotenone group compared with those in the vehicle group. Compared to the rotenone control group, the rotenone + TTE (5 or 10 mg per kg) group showed significant decreases in 8-OHdG and MTH1 (*Fig. 7B* and *7C*).

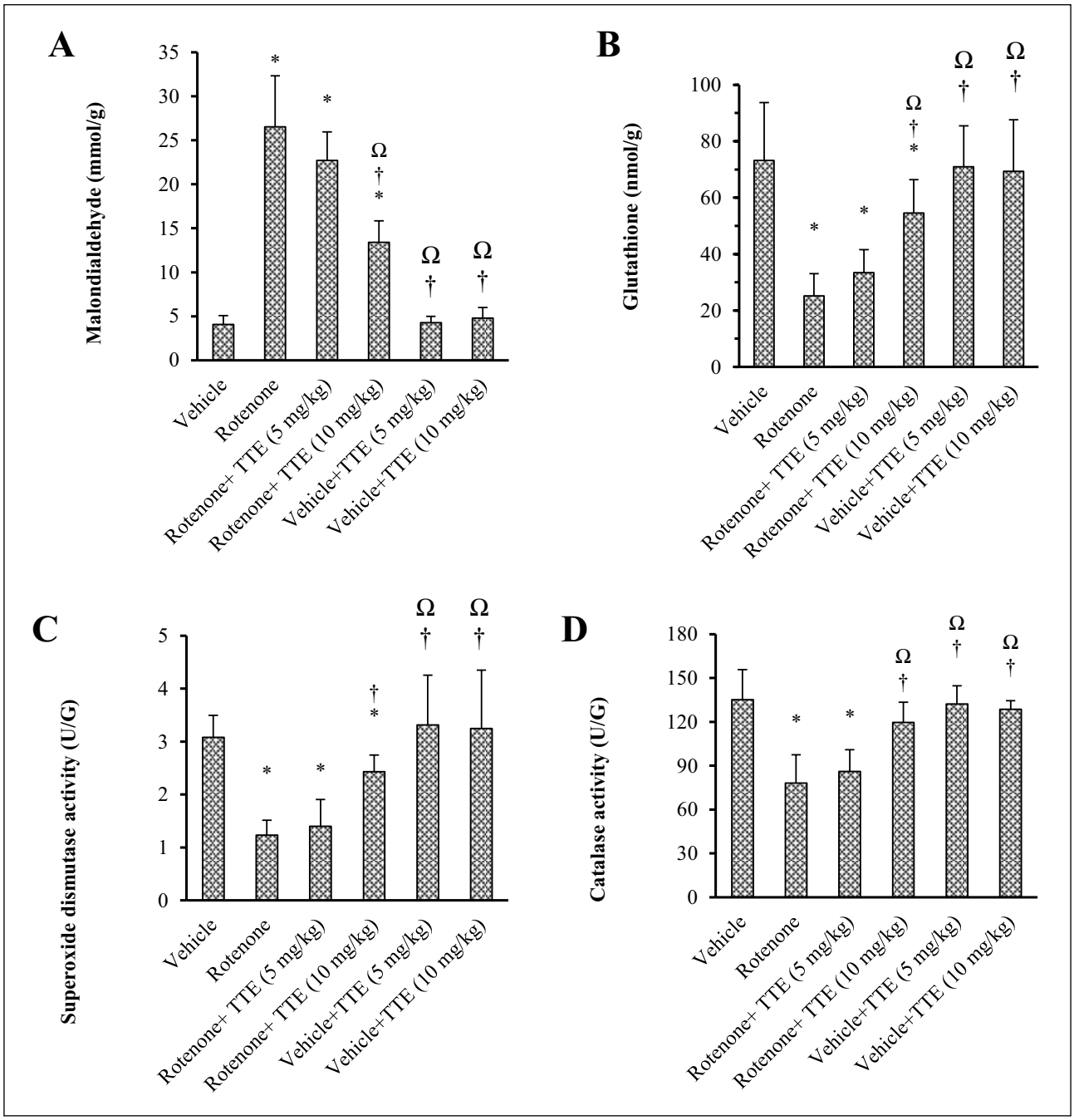

Fig. 6. Effect of *T. terrestris* extract (5 or 10 mg/kg) on oxidative stress biomarkers in striata of the study groups. Striatal level of malondialdehyde (A), reduced glutathione (B), superoxide dismutase activity (C) and catalase activity (D). Data are mean ± SD and were analyzed using one-way ANOVA and Tukey's test. P-value < 0.05 was set as the accepted level of significance. * Compared to vehicle group, † compared to rotenone group, Ω compared to rotenone + TTE (5 mg/kg) group.

DISCUSSION

The effectiveness of TTE was examined in the present study using the rotenone parkinsonian model, which recapitulates both the clinical symptoms and pathological abnormalities of PD and induces selective neurotoxicity to dopaminergic neurons (51). The current study elucidated a protective effect for TTE against rotenone induced neurodegeneration and highlighted a novel role of TTE in suppressing oxidative DNA damage and $CD_{11}b$ expression.

In this study, rotenone injection into mice induced a parkinsonian-like phenotype. This phenotype was demonstrated by the impaired locomotor function assessed in two well-documented behavioral tests, the pole test and open-field tests. Furthermore, histopathological examination revealed greater number of pyknotic neurons while immunohistochemistry indicated lower percentage of TH-positive neurons. Moreover, biochemical analyses revealed a decrease in striatal dopamine and GSH as well as a rise in lipid peroxidation, inflammatory markers, DNA damage and expression of the microglia antigen, CD11b.

According to previous studies, rotenone injection in rodents leads to impairments in locomotor activity in many behavioral paradigms such as the open-field test (19, 37, 52), pole test (4),

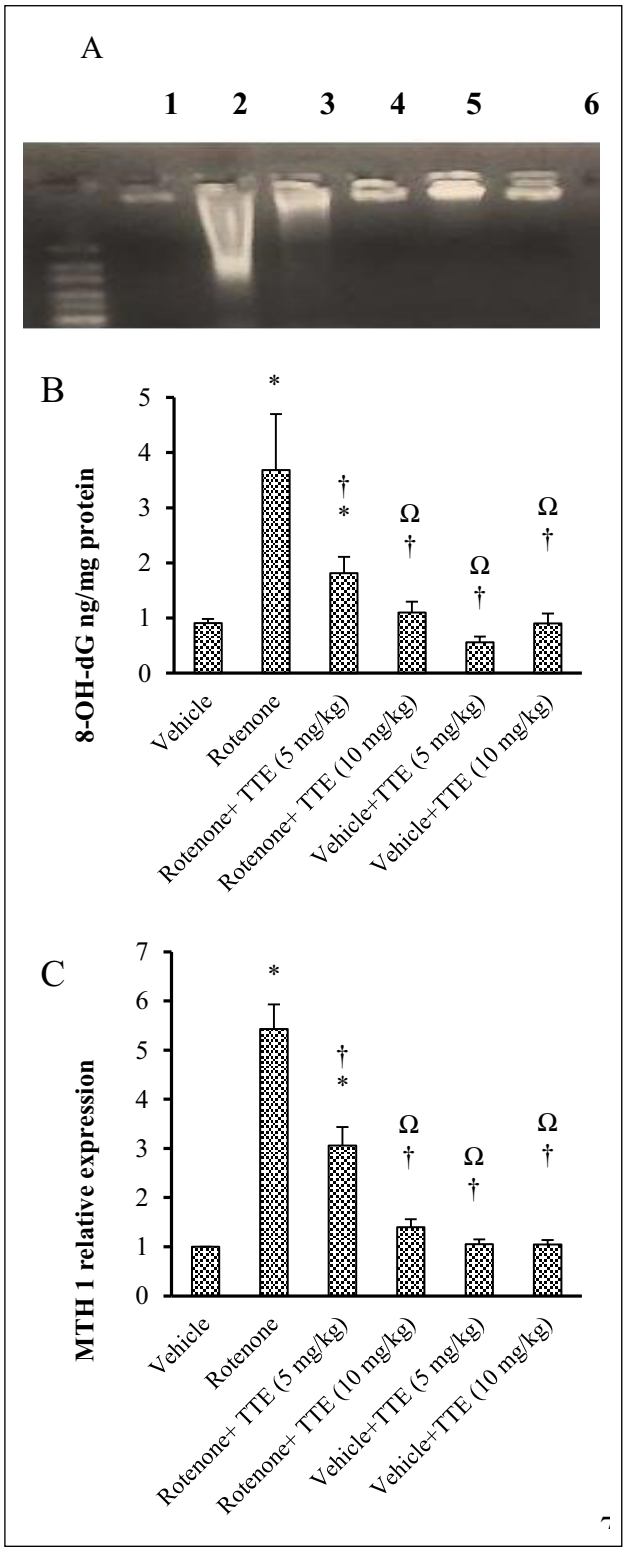

Fig. 7. Effect of *T. terrestris* extract (5 or 10 mg/kg) on DNA damage. (A): DNA laddering assay: 1) a ladder for vehicle group, 2) a ladder from rotenone group, 3) and 4) ladders from rotenone + TTE (5 and 10 mg/kg) groups. 5) and 6) ladders from mice received *per se* treatment with *T. terrestris* extract (10 mg per kg). (B): Assay for 8-OH-dG and (C): MTH1 in striatal samples Data are mean ± SD and were analyzed using one-way ANOVA and Tukey's test. P-value < 0.05 was set as the accepted level of significance. * Compared to vehicle group, † compared to rotenone group, Ω compared to rotenone + TTE (5 mg/kg) group.

rotarod test (18, 19), rears test (29, 30), catalepsy test (6, 53), grid test (30) and stepping test (54). Rotenone also reportedly increases anxiety-like behavior in mice tested in the elevated plus maze (55).

Under normal conditions, neurons containing TH are responsible for catalysis and converting L-tyrosine to DOPA (56). TH is a cytosolic enzyme in catecholamine-containing cells and is depleted in conditions of neuronal toxicity among dopaminergic neurons (56). Depending on the decline in TH, neurotoxicity was markedly apparent in the SN following rotenone treatment. Our finding was consistent with a previous study in which systemic treatment with rotenone was administered for two months reducing TH in the striatum and caudate putamen (57) and depleting TH in the SN neurons (4, 6).

It is mostly important to consider that the crosstalk between inflammation and oxidative stress rises proportional with age, which results in the accumulation of malfunctioning mitochondria and more ROS (58). The accumulation of ROS leads to cell damage and subsequent activation of inflammatory mediators which ultimately results in a state of cellular senescence (59). Senescent cells release pro-inflammatory cytokines (60). In human parkinsonism, the endless generation of ROS through autoxidation and MAO metabolism for dopamine and the existence of iron and low GSH levels were detected in the SNpc compared to those in other brain areas (61, 62). In PD, an increase in oxidative damage to DNA in nuclei and mitochondria was detected in SN dopamine-producing neurons (63).

In the current study, rotenone parkinsonian mice showed striatal DNA fragmentation and increases in striatal 8-OHdG levels and MTH1 expression. Similarly, oxidative DNA damage in the form of oxidized guanine is retained in the mitochondrial and nuclear DNA of dopamine-producing neurons of the SN in PD (64). Furthermore, 8-OHdG dramatically increased in post-mortem samples of the SN from parkinsonian brains (17, 65). As a result of oxidative stress, the content of common deletions in mitochondrial DNA increased in the few surviving dopamine producing neurons in the parkinsonian SN (66).

The MTH1 gene encodes 8-oxo-7,8-dihydrodeoxyguanosine triphosphatase (8-oxodGTPase) that hydrolyzes 8-oxo-2'-deoxyguanosine-5'-triphosphate (8-oxodGTP) moieties (67). In rodent and human cells, MTH1 hydrolyzes oxidized purines to avoid their incorporation into DNA or RNA. MTH1 is thought to play a crucial role in halting cytotoxicity of oxidized purines (68). Furthermore, 1-methyl-4-phenyl-1,2,3,6-tetrahydropyridine administered in MTH1-null mice resulted in greater increase of 8-oxoguanine in mitochondrial DNA from in striatum; this accumulation was accompanied by greater neuronal dysfunction than that detected in the wild-type mice (69).

One study with MTH1-deficient cells published that MTH1 lessens the buildup of 8-oxo-guanine in nuclear and mitochondrial DNA from mouse brain (70), therefore, protecting the brain from oxidative stress. Consistently, MTH1-null mouse fibroblasts had high susceptibility to H_2O_2-induced cell death accompanied by an ongoing accumulation of 8-oxo-guanine in nuclear and mitochondrial DNA (71). In previous studies, cortical neurons prepared from MTH1 (8-oxo-dGTPase)/OGG1 (8-oxoG DNA glycosylase)-double deficient adult mouse brains exhibited reduced *in vitro* neuritogenesis (72). In another study, transgenic expression of human MTH1 inhibited the neurodegenerative process by halting accumulation of 8-oxo-7,8-dihydroguanine in neuronal mitochondrial genomes, indicating that upregulation of MTH1 expression may be useful for neurons (73).

Similar to the current study, some previous reports indicated that rotenone-induced parkinsonism is associated with oxidative impairment. For instance, one study indicated that systemic

administration of rotenone led to an increase in cortical and striatal protein carbonyls and reduced hippocampal total thiols in mice (55). Another study indicated significant increases in cerebellar and striatal levels of ROS, MDA, hydroperoxides and NO levels in addition to significant decreases in activity levels of antioxidant enzymes, the levels of GSH, acetylcholinesterase and mitochondrial dysfunctions. The two studies confirmed a state of oxidative stress (74).

One research team inspected the alterations in metallothionein expression by systemic administration of rotenone for 6 weeks in the striatum of C57BL mice. The authors found greater expression of metallothioneins, which are thought to defend dopaminergic neurons against oxidative stress, with astrocyte activation in the striatum (75). *One in vitro* study revealed that compared with the blank control, 1 μM rotenone treatment in BV2 microglia significantly increased intracellular ROS by approximately 1.99-fold (76). Similarly, rotenone reportedly increased MDA levels and protein oxidation in cell and Drosophila models of PD (77).

Glia cells protect neurons from damage. Thus, glial cells are targeted by numerous insults in the nervous system (78). The current results indicated that rotenone injection in mice led to activation of microglia cells as demonstrated by upregulation of CD11b expression. Neuronal damage in PD is linked to a chronic state of inflammation (79) as well as reactive microgliosis and astrogliosis (80). Activation of microglia may underlie the oxidative injury that contributes to neurotoxicity of rotenone (78). Various enzymes, like NADPH oxidase, are activated in microglia and produce ROS that initiate redox signaling and in turn intensify the pro-inflammatory cascade (81).

Since the SN contains a high density of microglial cells, reactive microglia have been associated with the selective neurodegeneration observed in PD (82, 83). *In vitro*, rotenone-induced activation of microglia occurred prior to obvious neurodegeneration (84). Furthermore, rotenone recapitulates the glial pathology detected during parkinsonism, including selective and widespread activation of microglia in the SN (51). Microglia respond to pro-inflammatory generators by changing to an activated phenotype, leading to an alteration of cellular function towards releasing cytotoxic factors directed at destructing attacking pathogens (85, 86). Hence, the existence of active microglia is a valuable marker of current neuronal injury (87).

Experimental and clinical studies consider neuroinflammation is implicated in neurodegeneration and neuropsychiatric dysfunction subsequent to single or repetitive traumatic injury to brain (88-91). Microglia and inflammatory neurodegeneration are believed to be involved in hypoxia (92), stroke (93) and neuropathic pain (94). In PD, many studies propose that activated microglia participate in the progressive nature (95) and implicate the immune system (96). A large observational study involving 4026 PD cases and 15969 matched controls concluded that chronic use of acetaminophen or aspirin was not linked to a noticeably changed risk of parkinsonism (97).

McGeer *et al*. provided the first evidence on activation of microglia in the SNpc of parkinsonian brains (98). Unfortunately, post-mortem findings cannot reveal the initiation of microglial activation in the pathology of PD. A recent PET imaging study using isoqunoline, [11C](R)-PK11195, with the ability to bind to peripheral benzodiazepine receptors produced by active microglia, have demonstrated microglial reactivity during early-stage PD (99). In addition, microglial activation and damage to midbrain dopaminergic terminals were correlated. Furthermore, microglial activation in the PD brain was proven to increase pro-inflammatory cytokine expression (100).

Striatal iNOS expression was upregulated in rotenone-treated mice. Our results agree with those of previous reports (53, 101), which indicated that activation of NOS and overproduction of peroxynitrite ions may contribute to PD pathogenesis. Additionally, a community-based case-control study detected a relationship between PD and iNOS gene polymorphisms (102). In contrast, Huerta *et al*. did not discover a link between PD and polymorphisms in genes encoding eNOS, nNOS and iNOS (103). In addition, NOS-expressing genes have been described to produce excess amounts of NO, which underlies neurodegeneration in PD (104). The expression of iNOS reportedly inversely correlated with TH immunolabeling (105).

Currently, traditional medicinal plants are utilized worldwide for various diseases. The study of these medicines might offer a way to find new medications for PD (106). In the present study, the outcome of administration of TTE for 17 days on locomotor dysfunction was tested and considerable improvements were found. Moreover, TTE-treated mice displayed a significant rise in their nigrostriatal dopamine levels. In context, results showed the decreased numbers of TH-positive cells was ameliorated by TTE.

Moreover, mice treated with the higher dose of TTE displayed a decline in MDA levels with increases in GSH, CAT and SOD, which revealed that TTE protected against oxidative damage. Similarly, a myocardial protective action of tribulosin was documented against ischemic/reperfusion injury through antioxidant and antiapoptotic effect (107). These findings agree with those claimed that TTE protects against lipid peroxidation in diabetic rats (23). Furthermore, TTE protects against mercuric chloride nephrotoxicity in mice through anti-oxidative effects by modulating MDA, GSH, SOD and CAT (22). TTE also decreased hypoxia-reoxygenation induced apoptosis in rat cortical neurons (108). Other findings support the protective privileges of TTE on cerebral architecture in a rabbit model of diet-induced hyperlipidemia (109). In accordance, TTE reportedly exerts a neuroprotective effect in rats exposed to middle cerebral artery occlusion that was mediated by inhibition of inflammatory mediators (110). In accordance, the mechanisms of gross saponins of TT against myocardial apoptosis were confirmed to be linked to inhibition of the mitochondrial apoptosis pathway (111). Another study confirmed that TTE ameliorates ischemic insults in a cell-based (H9c2) myocardial ischemia model by safeguarding mitochondrial function (112).

As revealed in the present study, TTE exerted an influence on microglia as demonstrated by a reduction in the expression of CD11b, iNOS and COX-2 mRNA levels. Hence, we illustrated a neuroprotective role of *T. terrestris* against rotenone-induced neurodegeneration *via* suppression of microglial activation. One previous study showed that TTE inhibits COX-2 activity in cultured mouse macrophage cells exposed to lipopolysaccharides (25).

In conclusion, the current study provided evidence that oxidative damage in nucleic acid is a key risk factor for experimental PD in mice. The current findings document a novel neuroprotective role for TTE in rotenone parkinsonian mice. This action was, at least in part, related to the antioxidant and anti-inflammatory action of TTE. Furthermore, we verified the influence of TTE in suppressing microglial activation as a target for the alleviation of neuronal damage in the rotenone PD model.

This study was carried out at Suez Canal University, Ismailia, Egypt.

Acknowledgements: Authors wish to acknowledge the Egyptian Knowledge Bank for facilitating the language editing process for this article *via* Springer-Nature.

Conflict of interests: None declared.

REFERENCES

1. Dauer W, Przedborski S. Parkinson's disease: mechanisms and models. *Neuron* 2003; 39: 889-909.
2. Gopalakrishna A, Alexander SA. Understanding Parkinson disease: a complex and multifaceted illness. *J Neurosci Nurs* 2015; 47: 320-326.
3. Krzymowski T, Stefanczyk-Krzymowska S. New facts and the concept of physiological regulation of the dopaminergic system function and its disorders. *J Physiol Pharmacol* 2015; 66: 331-341.
4. Zaitone SA, Ahmed E, Elsherbiny NM, *et al*. Caffeic acid improves locomotor activity and lessens inflammatory burden in a mouse model of rotenone-induced nigral neurodegeneration: relevance to Parkinson's disease therapy. *Pharmacol Rep* 2019; 71: 32-41.
5. Ferris CF, Marella M, Smerkers B, *et al*. A phenotypic model recapitulating the neuropathology of Parkinson's disease. *Brain Behav* 2013; 3: 351-366.
6. Teema AM, Zaitone SA, Moustafa YM. Ibuprofen or piroxicam protects nigral neurons and delays the development of L-dopa induced dyskinesia in rats with experimental parkinsonism: influence on angiogenesis. *Neuropharmacology* 2016; 107: 432-450.
7. Madabhushi R, Pan L, Tsai L-H. DNA damage and its links to neurodegeneration. *Neuron* 2014; 83: 266-282.
8. Dolle Christian, Flones Irene, Nido GS, *et al*. Defective mitochondrial DNA homeostasis in the substantia nigra in Parkinson disease. *Nat Commun* 2016; 7: 13548. doi: 10.1038/ncomms13548
9. Al Dera H. Neuroprotective effect of resveratrol against late cerebral ischemia reperfusion induced oxidative stress damage involves upregulation of osteopontin and inhibition of interleukin-1beta. *J Physiol Pharmacol* 2017; 68: 47-56.
10. Soni H, Pandya G, Patel P, Acharya A, Jain M, Mehta A. A beneficial effects of carbon monoxide-releasing molecule-2 (corm-2) on acute doxorubicin cardiotoxicity in mice: role of oxidative stress and apoptosis. *Toxicol Appl Pharmacol* 2011; 253: 70-80.
11. Gerhard A, Pavese N, Hotton G, *et al*. In vivo imaging of microglial activation with [11C](R)-PK11195 PET in idiopathic Parkinson's disease. *Neurobiol Dis* 2006; 21: 404-412.
12. Hirsch EC. Glial cells and Parkinson's disease. *J Neurol* 2000; 247: II58-II62.
13. Liu B, Gao HM, Wang JY, Jeohn GH, Cooper CL, Hong JS. Role of nitric oxide in inflammation-mediated neurodegeneration. *Ann NY Acad Sci* 2002; 962: 318-331.
14. Verdile G, Keane KN, Cruzat VF, *et al*. Inflammation and oxidative stress: the molecular connectivity between insulin resistance, obesity, and Alzheimer's disease. Mediators Inflamm 2015; 2015: 105828. doi: 10.1155/2015/105828 2015
15. Bregeon D, Peignon PA, Sarasin A. Transcriptional mutagenesis induced by 8-oxoguanine in mammalian cells. *PLoS Genet* 2009; 5: e1000577. doi: 10.1371/journal.pgen.1000577
16. Gmitterova K, Gawinecka J, Heinemann U, Valkovic P, Zerr I. DNA versus RNA oxidation in Parkinson's disease: which is more important? *Neurosci Lett* 2018; 662: 22-28.
17. Nakabeppu Y, Tsuchimoto D, Yamaguchi H, Sakumi K. Oxidative damage in nucleic acids and Parkinson's disease. *J Neurosci Res* 2007; 85: 919-934.
18. Anusha C, Sumathi T, Joseph LD. Protective role of apigenin on rotenone induced rat model of Parkinson's disease: Suppression of neuroinflammation and oxidative stress mediated apoptosis. *Chem Biol Interact* 2017; 269: 67-79.
19. Zhang S, Shao SY, Song XY, *et al*. Protective effects of Forsythia suspense extract with antioxidant and anti-inflammatory properties in a model of rotenone induced neurotoxicity. *Neurotoxicology* 2016; 52: 72-83.
20. Warrier PK, Nambiar VPK. Indian Medicinal Plants: A Compendium of 500 Species. Orient Blackswan, 1993.
21. Gauthaman K, Adaikan PG, Prasad RN. Aphrodisiac properties of Tribulus Terrestris extract (Protodioscin) in normal and castrated rats. *Life Sci* 2002; 71: 1385-1396.
22. Kavitha AV, Jagadeesan G. Role of Tribulus terrestris (Linn.) (Zygophyllacea) against mercuric chloride induced nephrotoxicity in mice, Mus musculus (Linn.). *J Environ Biol* 2006; 27 (Suppl. 2): 397-400.
23. Amin A, Lotfy M, Shafiullah M, Adeghate E. The protective effect of Tribulus terrestris in diabetes. *Ann NY Acad Sci* 2006; 1084: 391-401.
24. Kianbakht S, Jahaniani F. Evaluation of antibacterial activity of Tribulus terrestris L. growing in Iran. *Iran J Pharmacol Ther* 2003; 2: 22-30.
25. Hong CH, Hur SK, Oh OJ, Kim SS, Nam KA, Lee SK. Evaluation of natural products on inhibition of inducible cyclooxygenase (COX-2) and nitric oxide synthase (iNOS) in cultured mouse macrophage cells. *J Ethnopharmacol* 2002; 83: 153-159.
26. Deole YS, Chavan SS, Ashok BK, Ravishankar B, Thakar AB, Chandola HM. Evaluation of anti-depressant and anxiolytic activity of Rasayana Ghana Tablet (A compound Ayurvedic formulation) in albino mice. *Ayu* 2011; 32: 375-379.
27. Zhu W, Du Y, Meng H, Dong Y, Li L. A review of traditional pharmacological uses, phytochemistry, and pharmacological activities of Tribulus terrestris. *Chem Cent J* 2017; 11: 60. doi: 10.1186/s13065-017-0289-x
28. Rolland T, Tasan M, Charloteaux B, *et al*. A proteome-scale map of the human interactome network. *Cell* 2014; 159: 1212-1226.
29. Johnson ME, Bobrovskaya L. An update on the rotenone models of Parkinson's disease: Their ability to reproduce the features of clinical disease and model gene-environment interactions. *Neurotoxicology* 2015; 46: 101-116.
30. Zhang ZN, Zhang JS, Xiang J, *et al*. Subcutaneous rotenone rat model of Parkinson's disease: dose exploration study. *Brain Res* 2017; 1655: 104-113.
31. Farahani MS, Bahramsoltani R, Farzaei MH, Abdollahi M, Rahimi R. Plant-derived natural medicines for the management of depression: an overview of mechanisms of action. *Rev Neurosci* 2015; 26: 305-321.
32. Phillips OA, Mathew KT, Oriowo MA. Antihypertensive and vasodilator effects of methanolic and aqueous extracts of Tribulus terrestris in rats. *J Ethnopharmacol* 2006; 104: 351-255.
33. Al-Ali M, Wahbi S, Twaij H, Al-Badr A. Tribulus terrestris: preliminary study of its diuretic and contractile effects and comparison with Zea mays. *J Ethnopharmacol* 2003; 85: 257-260.
34. Matsuura K, Kabuto H, Makino H, Ogawa N. Pole test is a useful method for evaluating the mouse movement disorder caused by striatal dopamine depletion. *J Neurosci Methods* 1997; 73: 45-48. Doi: 10.1016/S0165-0270(96)02211-X.
35. Ogawa N, Hirose Y, Ohara S, Ono T, Watanabe Y. A simple quantitative bradykinesia test in MPTP-treated mice. *Res Commun Chem Pathol Pharmacol* 1985; 50: 435-441.
36. Fleming SM, Salcedo J, Fernagut PO, *et al*. Early and progressive sensorimotor anomalies in mice overexpressing wild-type human α-synuclein. *J Neurosci* 2004; 24: 9434-9440.
37. Khatri DK, Juvekar AR. Neuroprotective effect of curcumin as evinced by abrogation of rotenone-induced motor deficits,

oxidative and mitochondrial dysfunctions in mouse model of Parkinson's disease. *Pharmacol Biochem Behav* 2016; 150-151: 39-47.
38. Leite-Almeida H, Almeida-Torres L, Mesquita AR, *et al*. The impact of age on emotional and cognitive behaviours triggered by experimental neuropathy in rats. *Pain* 2009; 144: 57-65.
39. Magnani P, Conforti A, Zanolin E, Marzotto M, Bellavite P. Dose-effect study of Gelsemium sempervirens in high dilutions on anxiety-related responses in mice. *Psychopharmacology* (*Berl*) 2010; 210: 533-545.
40. Xu YL, Reinscheid RK, Huitron-Resendiz S, *et al*. Neuropeptide S: a neuropeptide promoting arousal and anxiolytic-like effects. *Neuron* 2004; 43: 487-497.
41. Alhaj MW, Zaitone SA, Moustafa YM. Fluvoxamine alleviates seizure activity and downregulates hippocampal GAP-43 expression in pentylenetetrazole-kindled mice: role of 5-HT3 receptors. *Behav Pharmacol* 2015; 26: 369-382.
42. Wu D, Xie H, Lu H, Li W, Zhang Q. Sensitive determination of norepinephrine, epinephrine, dopamine and 5-hydroxytryptamine by coupling HPLC with [Ag(HIO6)2]5-luminol chemiluminescence detection. *Biomed Chromatogr* 2016; 30: 1458-1466.
43. Tammimaki A, Aonurm-Helm A, Kaenmaki M, Mannisto PT. Elimination of extracellular dopamine in the medial prefrontal cortex of conscious mice analysed using selective enzyme and uptake inhibitors. *J Physiol Pharmacol* 2016; 67: 301-309.
44. Ohkawa H, Ohishi N, Yagi K. Assay for lipid peroxides in animal tissues by thiobarbituric acid reaction. *Anal Biochem* 1979; 95: 351-358.
45. Beutler E, Duron O, Kelly BM. Improved method for the determination of blood glutathione. *J Lab Clin Med* 1963; 61: 882-888.
46. Kakkar P, Das B, Viswanathan PN. A modified spectrophotometric assay of superoxide dismutase. *Indian J Biochem Biophys* 1984; 21: 130-132.
47. Aebi H. Catalase in vitro. *Methods Enzymol* 1984: 105: 121-126.
48. Tomita K, Freeman BL, Bronk SF, *et al*. CXCL10-mediates macrophage, but not other innate immune cells-associated inflammation in murine nonalcoholic steatohepatitis. *Sci Rep* 2016; 6: 28786. doi: 10.1038/srep28786
49. Gan L, Liu Z, Cao W, Zhang Z, Sun C. FABP4 reversed the regulation of leptin on mitochondrial fatty acid oxidation in mice adipocytes. *Sci Rep* 2015; 5: 13588. doi: 10.1038/srep13588
50. Webb LM, Lundie RJ, Borger JG, *et al*. Type I interferon is required for T helper (Th) 2 induction by dendritic cells. *EMBO J* 2017; 36: 2404-24-2418.
51. Sherer TB, Kim JH, Betarbet R, Greenamyre JT. Subcutaneous rotenone exposure causes highly selective dopaminergic degeneration and α-synuclein aggregation. *Exp Neurol* 2003; 179: 9-16.
52. Wu F, Wang Z, Gu JH, Ge JB, Liang ZQ, Qin ZH. p38MAPK/p53-mediated Bax induction contributes to neurons degeneration in rotenone-induced cellular and rat models of Parkinson's disease. *Neurochem Int* 2013; 63: 133-140.
53. Xiong ZK, Lang J, Xu G, *et al*. Excessive levels of nitric oxide in rat model of Parkinson's disease induced by rotenone. *Exp Ther Med* 2015; 9: 553-558.
54. Naughton C, O'Toole D, Kirik D, Dowd E. Interaction between subclinical doses of the Parkinson's disease associated gene, α-synuclein, and the pesticide, rotenone, precipitates motor dysfunction and nigrostriatal neurodegeneration in rats. *Behav Brain Res* 2017; 316: 160-168.
55. Gokul K, Muralidhara. Oral supplements of Aqueous extract of tomato seeds alleviate motor abnormality, oxidative impairments and neurotoxicity induced by rotenone in mice: relevance to Parkinson's disease. *Neurochem Res* 2014; 39: 1382-1394.
56. Kaufman S. Tyrosine hydroxylase. *Adv Enzymol Relat Areas Mol Biol* 1995; 70: 103-220.
57. Alam M, Schmidt WJ. Rotenone destroys dopaminergic neurons and induces parkinsonian symptoms in rats. *Behav Brain Res* 2002; 136: 317-324.
58. Lionaki E, Gkikas I, Tavernarakis N. Differential protein distribution between the nucleus and mitochondria: implications in aging. *Front Genet* 2016; 7: 162. doi: 10.3389/fgene.2016.00162
59. Lopez-Otin C, Blasco MA, Partridge L, Serrano M, Kroemer G. The hallmarks of aging. *Cell* 2013; 153: 1194-1217.
60. Fougere B, Delrieu J, Campo N, Soriano G, Sourdet S, Vellas B. Cognitive frailty: mechanisms, tools to measure, prevention and controversy. *Clin Geriatr Med* 2017; 33: 339-355.
61. Berg D, Youdim MB, Riederer P. Redox imbalance. *Cell Tissue Res* 2004; 318: 201-213.
62. Jenner P. Oxidative stress in Parkinson's disease. *Ann Neurol* 2003; 53 (S3): S26-S38.
63. Sherer TB, Greenamyre JT. Oxidative damage in Parkinson's disease. *Antioxid Redox Signal* 2005; 7: 627-629.
64. Basu S, Je G, Kim YS. Transcriptional mutagenesis by 8-oxodG in α-synuclein aggregation and the pathogenesis of Parkinson's disease. *Exp Mol Med* 2015; 47: e179. doi: 10.1038/emm.2015.54
65. Alam ZI, Jenner A, Daniel SE, *et al*. Oxidative DNA damage in the Parkinsonian brain: an apparent selective increase in 8-hydroxyguanine levels in substantia nigra. *J Neurochem* 1997; 69: 1196-1203.
66. Bender A, Krishnan KJ, Morris CM, *et al*. High levels of mitochondrial DNA deletions in substantia nigra neurons in aging and Parkinson disease. *Nat Genet* 2006; 38: 515-517.
67. Risom L, Moller P, Loft S. Oxidative stress-induced DNA damage by particulate air pollution. *Mutat Res Mol Mech Mutagen* 2005; 592: 119-137.
68. Nakabeppu Y, Kajitani K, Sakamoto K, Yamaguchi H, Tsuchimoto D. MTH1, an oxidized purine nucleoside triphosphatase, prevents the cytotoxicity and neurotoxicity of oxidized purine nucleotides. *DNA Repair* 2006; 5: 761-772.
69. Yamaguchi H, Kajitani K, Dan Y, *et al*. MTH1, an oxidized purine nucleoside triphosphatase, protects the dopamine neurons from oxidative damage in nucleic acids caused by 1-methyl-4-phenyl-1,2,3,6-tetrahydropyridine. *Cell Death Differ* 2006; 13: 551-563.
70. Kajitani K, Yamaguchi H, Dan Y, Furuichi M, Kang D, Nakabeppu Y. MTH1, an oxidized purine nucleoside triphosphatase, suppresses the accumulation of oxidative damage of nucleic acids in the hippocampal microglia during kainate-induced excitotoxicity. *J Neurosci* 2006; 26: 1688-1698.
71. Yoshimura D, Sakumi K, Ohno M, *et al*. An oxidized purine nucleoside triphosphatase, MTH1, suppresses cell death caused by oxidative stress. *J Biol Chem* 2003; 278: 37965-37973.
72. Abolhassani N, Leon J, Sheng Z, *et al*. Molecular pathophysiology of impaired glucose metabolism, mitochondrial dysfunction, and oxidative DNA damage in Alzheimer's disease brain. *Mech Ageing Dev* 2017; 161: 95-104.
73. Nakabeppu Y, Ohta E, Abolhassani N. MTH1 as a nucleotide pool sanitizing enzyme: friend or foe? *Free Radic Biol Med* 2017; 107: 151-158.

74. Manjunath MJ, Muralidhara. Effect of Withania somnifera supplementation on rotenone-induced oxidative damage in cerebellum and striatum of the male mice brain. *Cent Nerv Syst Agents Med Chem* 2013; 13: 43-56.
75. Murakami S, Miyazaki I, Sogawa N, Miyoshi K, Asanuma M. Neuroprotective effects of metallothionein against rotenone-induced myenteric neurodegeneration in parkinsonian mice. *Neurotox Res* 2014; 26: 285-298.
76. Liang Y, Jing X, Zeng Z, *et al*. Rifampicin attenuates rotenone-induced inflammation via suppressing NLRP3 inflammasome activation in microglia. *Brain Res* 2015; 1622: 43-50.
77. Pandareesh MD, Shrivash MK, Naveen Kumar HN, Misra K, Srinivas Bharath MM. Curcumin monoglucoside shows improved bioavailability and mitigates rotenone induced neurotoxicity in cell and Drosophila models of Parkinson's disease. *Neurochem Res* 2016; 41: 3113-3128.
78. Swarnkar S, Singh S, Goswami P, Mathur R, Patro IK, Nath C. Astrocyte activation: a key step in rotenone induced cytotoxicity and DNA damage. *Neurochem Res* 2012; 37: 2178-2189.
79. Barcia C, Barreiro AF, Poza M, Herrero M-T. Parkinson's disease and inflammatory changes. *Neurotox Res* 2003; 5: 411-417.
80. Schwarz J, Weis S, Kraft E, *et al*. Signal changes on MRI and increases in reactive microgliosis, astrogliosis, and iron in the putamen of two patients with multiple system atrophy. *J Neurol Neurosurg Psychiatry* 1996; 60: 98-101.
81. Block ML, Zecca L, Hong J-S. Microglia-mediated neurotoxicity: uncovering the molecular mechanisms. *Nat Rev Neurosci* 2007; 8: 57-69.
82. Kim WG, Mohney RP, Wilson B, Jeohn GH, Liu B, Hong JS. Regional difference in susceptibility to lipopolysaccharide-induced neurotoxicity in the rat brain: role of microglia. *J Neurosci* 2000; 20: 6309-6316.
83. Lawson LJ, Perry VH, Dri P, Gordon S. Heterogeneity in the distribution and morphology of microglia in the normal adult mouse brain. *Neuroscience* 1990; 39: 151-170.
84. Gao HM, Hong JS, Zhang W, Liu B. Distinct role for microglia in rotenone-induced degeneration of dopaminergic neurons. *J Neurosci* 2002; 22: 782-790.
85. Graeber MB, Streit WJ, Kreutzberg GW. The microglial cytoskeleton: vimentin is localized within activated cells in situ. *J Neurocytol* 1988; 17: 573-580.
86. Oehmichen M, Gruninger H, Gencic M. Experimental studies on kinetics and functions of monuclear phagozytes of the central nervous system. in: Malignant Lymphomas of the Nervous System; Jellinger K, Seitelberger F, (eds.). Berlin, Heidelberg, Springer 1975, pp. 285-290.
87. Kreutzberg GW. Microglia: a sensor for pathological events in the CNS. *Trends Neurosci* 1996; 19: 312-318.
88. Aungst SL, Kabadi SV, Thompson SM, Stoica BA, Faden AI. Repeated mild traumatic brain injury causes chronic neuroinflammation, changes in hippocampal synaptic plasticity, and associated cognitive deficits. *J Cereb Blood Flow Metab* 2014; 34: 1223-1232.
89. Sadana P, Coughlin L, Burke J, Woods R, Mdzinarishvili A. Anti-edema action of thyroid hormone in MCAO model of ischemic brain stroke: possible association with AQP4 modulation. *J Neurol Sci* 2015; 354: 37-45.
90. Loane DJ, Kumar A, Stoica BA, Cabatbat R, Faden AI. Progressive neurodegeneration after experimental brain trauma: association with chronic microglial activation. *J Neuropathol Exp Neurol* 2014; 73: 14-29.
91. Mouzon BC, Bachmeier C, Ferro A, *et al*. Chronic neuropathological and neurobehavioral changes in a repetitive mild traumatic brain injury model. *Ann Neurol* 2013; 75: 241-254.
92. Olson EE, McKeon RJ. Characterization of cellular and neurological damage following unilateral hypoxia/ischemia. *J Neurol Sci* 2004; 227: 7-19.
93. Morioka T, Kalehua AN, Streit WJ. Characterization of microglial reaction after middle cerebral artery occlusion in rat brain. *J Comp Neurol* 1993; 327: 123-132.
94. Tsuda M, Mizokoshi A, Shigemoto-Mogami Y, Koizumi S, Inoue K. Activation of p38 mitogen-activated protein kinase in spinal hyperactive microglia contributes to pain hypersensitivity following peripheral nerve injury. *Glia* 2003; 45: 89-95.
95. Cao JJ, Li KS, Shen YQ. Activated immune cells in Parkinson's disease. *J Neuroimmune Pharmacol* 2011; 6: 323-329.
96. German DC, Eagar T, Sonsalla PK. Parkinson's disease: a role for the immune system. *Curr Mol Pharmacol* 2011; Jun 15: PMID 21675953
97. Becker C, Jick SS, Meier CR. NSAID use and risk of Parkinson disease: a population-based case-control study. *Eur J Neurol* 2011; 18: 1336-1342.
98. McGeer PL, Itagaki S, Boyes BE, McGeer EG. Reactive microglia are positive for Hla-dr in the substantia nigra of Parkinson's and Alzheimer's disease brains. *Neurology* 1988; 38: 1285-1291.
99. Doorduin J, De Vries EF, Dierckx RA, Klein HC. PET imaging of the peripheral benzodiazepine receptor: monitoring disease progression and therapy response in neurodegenerative disorders. *Curr Pharm Des* 2008; 14: 3297-3315.
100. Sawada M, Imamura K, Nagatsu T. Role of cytokines in inflammatory process in Parkinson's disease. *J Neural Transm Suppl* 2006; (70): 373-381.
101. Ebadi M, Sharma SK, Ghafourifar P, Brown-Borg H, El Refaey H. Peroxynitrite in the pathogenesis of Parkinson's disease and the neuroprotective role of metallothioneins. *Methods Enzymol* 2005; 396: 276-298.
102. Levecque C, Elbaz A, Clavel J, *et al*. Association between Parkinson's disease and polymorphisms in the nNOS and iNOS genes in a community-based case-control study. *Hum Mol Genet* 2003; 12: 79-86.
103. Huerta C, Sanchez-Ferrero E, Coto E, *et al*. No association between Parkinson's disease and three polymorphisms in the eNOS, nNOS, and iNOS genes. *Neurosci Lett* 2007; 413: 202-205.
104. Hancock DB, Martin ER, Vance JM, Scott WK. Nitric oxide synthase genes and their interactions with environmental factors in Parkinson's disease. *Neurogenetics* 2008; 9: 249-262.
105. Singh S, Das T, Ravindran A, *et al*. Involvement of nitric oxide in neurodegeneration: a study on the experimental models of Parkinson's disease. *Redox Rep* 2005; 10: 103-109.
106. Shahpiri Z, Bahramsoltani R, Hosein Farzaei FM, Farzaei F, Rahimi R. Phytochemicals as future drugs for Parkinson's disease: a comprehensive review. *Rev Neurosci* 2016; 27: 651-668.
107. Zhang S, Li H, Yang SJ. Tribulosin protects rat hearts from ischemia/reperfusion injury. *Acta Pharmacol Sin* 2010; 31: 671-678.
108. Liu XM, Huang QF, Zhang YL, Lou JL, Liu HS, Zheng H. Effects of Tribulus terrestris L. saponion on apoptosis of cortical neurons induced by hypoxia-reoxygenation in rats. [in Chinese] *Zhong Xi Yi Jie He Xue Bao* 2008; 6: 45-50.
109. Berkman Z, Tanriover G, Acar G, Sati L, Altug T, Demir R. Changes in the brain cortex of rabbits on a cholesterol-rich diet following supplementation with a herbal extract of Tribulus terrestris. *Histol Histopathol* 2009; 24: 683-692.

110. Jiang EP, Li H, Chen JG, Yang SJ. Protection by the gross saponins of Tribulus terrestris against cerebral ischemic injury in rats involves the NF-κB pathway. *Acta Pharm Sin B* 2011; 1: 21-26.
111. Wang SS, Ji YS, Li H, Yang SJ. Mechanisms of gross saponins of Tribulus terrestris via activating PKCepsilon against myocardial apoptosis induced by oxidative stress. [in Chinese]. *Yao Xue Xue Bao* 2009; 44: 134-139.
112. Reshma PL, Sainu NS, Mathew AK, Raghu KG. Mitochondrial dysfunction in H9c2 cells during ischemia and amelioration with Tribulus terrestris L. *Life Sci* 2016; 152: 220-230.

Received: June 25, 2018
Accepted: December 30, 2018

Author's address: Dr. Sawsan A Zaitone, Department of Pharmacology and Toxicology, Faculty of Pharmacy, Suez Canal University, Ismailia, Egypt; Current address: Faculty of Pharmacy, University of Tabuk, Tabuk, Saudi Arabia.
E-mail: sawsan_zaytoon@pharm.suez.edu.eg